



Published in final edited form as:

J Proteome Res. 2011 February 4; 10(2): 856–868. doi:10.1021/pr101006u.

Annotation and Structural Analysis of Sialylated Human Milk Oligosaccharides

Shuai Wu¹, Rudolf Grimm^{3,4}, J. Bruce German⁴, and Carlito B. Lebrilla^{*,1,2}

¹Department of Chemistry, University of California, Davis, CA 95616

²Department of Biochemistry and Molecular Medicine, School of Medicine, University of California, Davis, CA 95616

³Agilent Technologies Inc., Santa Clara, CA 95051

⁴Robert Mondavi Institute for Wine and Department of Food Science and Technology, University of California, Davis, CA 95616

Abstract

Sialylated human milk oligosaccharides (SHMOs) are important components of human milk oligosaccharides. Sialic acids are typically found on the nonreducing end and are known binding sites for pathogens and aid in neonates' brain development. Due to their negative charge and hydrophilic nature, they also help modulate cell-cell interactions. It has also been shown that sialic acids are involved in regulating the immune response and aid in brain development. In this study, the enriched SHMOs from pooled milk sample were analyzed by HPLC-Chip/QTOF MS. The instrument employs a microchip-based nano-LC column packed with porous graphitized carbon (PGC) to provide excellent isomer separation for SHMOs with highly reproducible retention time. The precursor ions were further examined with collision-induced dissociation (CID). By applying the proper collision energy, isomers can be readily differentiated by diagnostic peaks and characteristic fragmentation patterns. A set of 30 SHMO structures with retention times, accurate masses and MS/MS spectra was deduced and incorporated into an HMO library. When combined with previously determined neutral components, a library with over 70 structures is obtained allowing high-throughput oligosaccharide structure identification.

Keywords

Sialylated Human Milk Oligosaccharides; HPLC-Chip/QTOF MS; CID; Structure identification

Introduction

Human milk oligosaccharides (HMOs) have been known to have many biological functions including as prebiotics for stimulating the growth of beneficial intestinal bacteria, as receptor analogs to inhibit the binding of pathogens, and as components involved in

To whom correspondence should be addressed: Carlito B. Lebrilla, cblebrilla@ucdavis.edu; Tel: +1-530-752-0504; Fax: +1-530-752-8995.

Supporting Information Available:

MALDI FTICR-MS spectrum of enriched SHMOs in the negative ion mode with the list of monosaccharide compositions; MS/MS spectra of FS-LNH and FS-LNnH I in the positive ion mode; Quantitative analysis of sialylated HMOs based on the abundances from HPLC Chip/TOF MS; The deconvoluted data of 70 SHMOs found in enriched sample including accurate masses, monosaccharide composition, and retention times; The optimized conditions for exoglycosidase digestion. This information is available free of charge via the Internet at <http://pubs.acs.org/>.

modulating the immune system.¹⁻⁵ Sialic acids are important components of HMOs and are often found on the non-reducing termini of HMOs. Sialylated HMOs (SHMOs) constitute about 20% of all HMOs.⁶⁻⁷ They serve as binding sites for specific pathogens and toxins.^{1, 4, 8-10} For example, *in vitro* studies have shown that SHMOs significantly decrease the binding of leukocyte to endothelial cells while the neutral HMOs had no effect.⁷ Sialic acids, due to their negative charge and hydrophilic nature, help modulate the cell-cell interaction.¹¹ It is also believed that sialic acids serve as ligands for lectin binding involved in regulating the immune response.¹²⁻¹³ In addition, the brain is the organ with the highest level of sialic acids where it plays an important role in facilitating neuronal sprouting and plasticity.^{8, 14-15} SHMOs are therefore believed to play a key role in postnatal brain development.^{1, 4, 16-17}

Mass spectrometry provides the most sensitive and rapid method for characterizing SHMOs. Structure elucidation of SHMOs is generally more difficult than neutrals because sialic acids readily dissociate under many ionization conditions. A labile glycosidic bond is caused by the adjacent proton from the carboxylic acid group.¹⁸ In addition, the signal of SHMOs can be strongly suppressed by neutral HMOs.¹⁹ Derivatization of the acid group with methyl²⁰⁻²⁵ or other groups²⁶⁻²⁹ tended to stabilize the NeuAc moiety and enhance the sensitivity while decreasing fragmentation. The use of high performance liquid chromatography (HPLC) coupled to mass spectrometry eliminates many of the difficulties in analyzing sialylated oligosaccharides (OS). The separation of sialylated OS from the neutral minimizes the ion suppression. Furthermore, isomer separation with HPLC in conjunction with electrospray ionization, a soft ionization source, enhances the analysis of SHMO. Reversed phase column was studied for separating the permethylated OS.^{22, 30} Normal phase chromatography was also used for separating derivatized³¹ or underivatized^{26, 32} OS. High pH anion-exchange chromatography (HPAEC) is also an option and provides adequate separation of OS, although it is generally not amenable for coupling to mass spectrometry (MS).³³⁻³⁵ However, we generally find porous graphitized carbon (PGC) to be the best stationary phase for separating native OS isomers.^{6, 36-40} LC-MS provides composition and structural information during OS profiling^{6, 41} and LC-MS/MS or tandem MS provides efficient differentiation of isomeric species.^{26, 38, 42-43} Fragmentation methods for analyzing sialylated OS currently include collision induced dissociation (CID),^{29, 44-47} infrared multiphoton dissociation (IRMPD),^{28, 48-49} ultraviolet photodissociation (UVPD),⁵⁰ electron capture dissociation (ECD),⁵¹ electron detachment dissociation (EDD)⁵² and high energy CID in tandem time-of-flight (TOF/TOF) instruments.^{23, 53-54}

This laboratory is in the process of creating an annotated library of HMOs for the rapid identification of HMO structures. We have already reported a set of neutral HMOs.³⁶ In this report, we catalog the sialylated oligosaccharides. HPLC-Chip/QTOF MS instrument is used for analyzing enriched SHMO samples. The instrument employs microchip based nano-LC column packed with PGC that provides excellent isomer separation for SHMOs with highly reproducible retention time (RT). The precursor ions were further fragmented with CID. By applying proper collision energy (CE), isomers can be readily differentiated by diagnostic peaks and characteristic fragmentation patterns.

Experimental Section

Reagents and Materials

The OS used in this study are from pooled human milk provided by milk banks in San Jose, CA and Austin, TX. HMOs were isolated from the milk using a previously described procedure involving defatting, chloroform/methanol extraction, ethanol precipitation, and evaporation.⁶ A sample enrichment step with solid phase extraction (SPE) employing graphitized carbon cartridge (GCC) was used before the analysis. GCC (150 mg bed weight,

4mL volume) were purchased from Alltech (Deerfield, IL). Sodium borohydride (98%) and 2, 5-dihydroxybenzoic acid (DHB) were obtained from Sigma–Aldrich (St. Louis, MO). Standard HMOs were purchased from Dextra Laboratories (Earley Gate, UK). $\alpha(1\text{--}2)$ -Fucosidase was obtained from EMD CALBIOCHEM (La Jolla, CA), $\beta(1\text{--}3)$ -galactosidase and $\alpha(2\text{--}3)$ -neuraminidase from New England Biolab (Beverly, MA), $\beta(1\text{--}4)$ -galactosidase from ProZyme (San Leandro, CA), and $\alpha(1\text{--}3,4)$ -fucosidase from Sigma–Aldrich (St. Louis, MO). The non-selective sialidase was purified and provided by Prof. David Mills from the Department of Viticulture and Enology in UC Davis. All reagents are of analytical or HPLC grade.

Oligosaccharide Reduction and Enrichment

The pooled HMO sample (50 mg in 250 μL nanopure water) was reduced by 250 μL of 1.0 M sodium borohydride in a water bath at 65 $^{\circ}\text{C}$ for 1.5 hours. The resulting product was desalted and purified by SPE-GCC. The SPE cartridge was first conditioned by 6 mL 80% acetonitrile (ACN) with 0.1% trifluoroacetic acid (TFA, v/v) and then 6 mL nanopure water. The desalting was performed by loading 1-mg sample to each cartridge and washed with 30 mL nanopure water. The HMOs were eluted with 6 mL 5% ACN in water (v/v), 6 mL 10% ACN in water (v/v), 6 mL 20% ACN in water (v/v) and 6 mL 40% ACN with 0.05% TFA. SHMOs were enriched by collecting the 40% eluent only. The sample was dried *in vacuo* and reconstituted with nanopure water before MS analysis.

Separation of SHMOs by HPLC

The enriched SHMOs were separated on an Agilent 1100 series HPLC instrument with hypercarb PGC column (100 mm \times 3.0 mm, 5 μm particle size) and detected with photodiode array detector at 206 nm and 254 nm. A 20 μL sample (about 0.05 mg/ μL) was injected and eluted by binary solvent (A) 3.0% ACN/water (v/v) with 0.1% formic acid and (B) 90% ACN/water (v/v) with 0.1% formic acid at the flow rate 0.35 mL/min and with a gradient of 0.0–1.0 min, 0% B; 1.1–6.0 min, 8% B; 6.0–60 min, 8–18% B; 60–70 min, 18–100% B; 70–80 min, 100% B. Sialylated HMOs were collected into 80 fractions with one minute per tube. The samples were dried *in vacuo* and reconstituted with 25 μL water before MALDI MS analysis.

MALDI FTICR MS

The HiRes MALDI FTICR (IonSpec, Irvine, CA) is composed of an external MALDI source with a pulsed 355 nm Nd:YAG laser, a hexapole ion guide and a FTICR cell with a 7.0 Tesla shielded superconducting magnet. 2, 5-Dihydroxybenzoic acid (DHB) was used as matrix (8 mg/160 μL in 50% ACN/water (v/v)) in both positive and negative mode. The HMOs (0.5 μL) were spotted on a 100-sample stainless steel plate with 0.5 μL matrix solution. In the positive mode, 0.25 μL , 0.01 μM NaCl solution was added as a cation dopant, while in the negative mode, no NaCl solution was added. The sample plate was dried in the vacuum chamber before MS analysis.

HPLC-Chip/TOF MS Analysis

The SHMOs samples were analyzed using the Agilent 6200 HPLC-Chip/TOF MS instrument (Agilent Technologies, Santa Clara, CA) with Agilent 1200 nano-LC and 6210 TOF MS. A detailed procedure was described in our previous paper.³⁶ The nano-LC was equipped with a capillary pump as the loading pump for sample enrichment, a nano-pump as the analytical pump for sample separation, a microwell-plate autosampler maintained at 6 $^{\circ}\text{C}$ by a thermostat, an Agilent HPLC-Chip cube interface and Agilent 6210 TOF MS. The micro-Chip consisted of an enrichment column with a volume of 40 nL and an analytical column 43 \times 0.075 mm i.d., which were both packed with PGC having 5 μm pore size. Both

pumps use binary solvent: **A** 3.0% ACN/water (v/v) with 0.1% formic acid and **B** 90% ACN/water (v/v) with 0.1% formic acid. A 4 $\mu\text{L}/\text{min}$ flow rate of solvent A was used for sample loading with 1 μL injection volume. A 45 minute gradient delivered by a nanoflow pump with a flow rate of 0.3 $\mu\text{L}/\text{min}$ was used for separation: 2.5–20.0 min, 0–16% B; 20.0–30.0 min, 16–44% B; 30.0–35.0 min, 44–100% B; 35.0–45.0 min, 100% B and a 20 minute equilibration time at 0% B.

Data analysis was performed with the Agilent MassHunter Qualitative Analysis software. The deconvoluted data file was calculated by an in-house software – “Oligosaccharide Calculator,” written in Igor Pro (Wavemetrics, Inc.). The output file included measured mass, calculated mass with mass error, and composition of each oligosaccharide sorted based on retention times and abundances. (Supplementary Table 1)

Twelve commercial OS standards were reduced and introduced into Chip/TOF under the identical condition in order to match the retention times and accurate masses with the corresponding OS in SHMO sample.³⁶

HPLC-Chip/QTOF MS Analysis

The Agilent HPLC-Chip/QTOF MS instrument (Agilent Technologies, Palo Alto, CA) is equipped with an Agilent 1200 series nano-LC system and Agilent 6520 QTOF coupled with a chip cube interface. The nano-LC system and the PGC chip used has been described above. Using the same injection volume, binary solvent and gradient, the resulting LC chromatograms in the Chip/QTOF were nearly identical to those of the Chip/TOF with minor variations of retention times. For both instruments, the same internal calibration technique was used to yield < 5 ppm mass accuracy for MS and < 20 ppm for MS/MS experiments.

In the positive ion mode, the data stored during the QTOF run included both centroid and profile. The instrument settings were adjusted during auto-tune and set to: fragmentor voltage 175 V, skimmer 65 V, and the octopole 1 RF voltage 750 V. The drying gas was heated at 325 °C with a flow rate of 5 L/min. The data acquisition was set to auto MS/MS with 2 spectra/s for MS scan and 1 spectra/s for MS/MS scan. The precursor ion was selected based on abundances with doubly-charged ion being given the first priority followed by singly-charged ion, triply-charged, and then other multiply-charged ions. A 4- m/z isolation window was used. All the calibrant ions were excluded from the isolation. The collision energy applied was based on the mass-to-charge (m/z) ratio of the ion with higher energy for larger ions. For this instrument, the collision energy was varied according to the equation:

$$CE(V) = \frac{(m/z)}{100(Da)} \times 1.3 - 3.5$$

where 1.3 is the slope and -3.5 is the y-intercept of the equation, both of which can be adjusted by the users, m/z is the mass-to-charge ratio of the precursor ion, CE is the collision energy. The equation was empirically determined by the manufacturer. In this study, the value of the slope and y-intercept were optimized to yield fragmentation that produced the most distinguishing features for each HMO isomer. The optimal collision energy for singly- and doubly-charged ions are expectedly different. For example, the collision energy applied to singly-charged ion of FS-LNH isomers (m/z 1512.6) is 16.2V, while 6.3V is used for the doubly-charged ion (m/z 756.8(+2)).

Exoglycosidase Digestion

Reaction buffer solutions were prepared with glacial acetic acid and 0.1 M ammonium acetate solution to the desired pH. 55–56 Enzymes were used without further purification. In a 0.2 mL PCR tube, 3 μ L buffer solution was added followed by 1 μ L OS sample and 1 μ L enzyme solution (mole ratio of protein to OS is about 1:100–200). The reaction mixture was incubated at 37 °C in a water bath. The reaction time used for each enzyme is tabulated in Supplementary Table 2.

Results

Enrichment and MALDI MS Profile of Sialylated OS from Human Milk

Sialylated OS make up about 20% of the total OS in human milk.^{6–7} To enrich the sialylated species, HMO mixtures were fractionated by SPE - GCC. Sialylated OS tend to elute with higher ratio of organic solvent, specifically 40% aqueous acetonitrile. Negative MALDI profile of the enriched mixture showed deprotonated ions and their monosaccharide compositions (Supplementary Figure 1). The compositions listed in the spectrum were assigned using an in-house software “Oligosaccharide Calculator” written in Igor (based on a mass accuracy < 5 ppm). The information provided by accurate mass showed that most of the SHMOs are monosialylated while only a small percentage is disialylated. The majority of the OS are also fucosylated with the number of fucoses (Fuc) ranging from one to four.

Chip/TOF MS Profile of Sialylated Components

Chip/TOF MS provides the online LC separation and MS detection with high mass accuracy. The PGC stationary phase is packed in a nanoflow column incorporated into a microchip with the electrospray tip integrated to minimize dead volume. The chip has been shown to yield excellent separation of OS isomers with highly reproducible retention times.^{6, 36} Since the separation is highly effective, α - and β -anomers at the reducing end have distinct retention times. To eliminate this complexity, the SHMOs were reduced to the alditol.^{6, 36}

Figure 1a is the base peak chromatogram (BPC) of the enriched SHMOs from a sample of pooled milk. Supplementary Table 1 shows the 70 SHMOs found along with their compositions and retention times. Most of the SHMOs are monosialylated and eluted after 20 minutes. SHMOs are generally eluted later than the neutral HMO. That isomers are effectively separated is illustrated in Figure 1b, which shows the extracted ion chromatogram (EIC) for the neutral mass 1511.6 (m/z 756.8 (+2), MS inset). For the convenience of this discussion, doubly-charged ions will be marked as +2 after the m/z , while the charge state for singly-charged ions will not be annotated. Supplementary Table 1 contains six different species (# 18 to 23) found by Chip/TOF with their monosaccharide compositions. Also included are the respective abundances sorted by RT. The neutral mass 1511.6 corresponds to one Fuc and one NeuAc on a lacto-*N*-hexaose core (FS-LNH). The composition belongs to seven isomers that are also the most abundant components.

The detailed procedure for elucidating their structures follows. To simplify the analysis, the mixture was separated using a standard HPLC into smaller pools of glycans, which were further analyzed individually. The HPLC column (100.0 mm \times 3.0 mm) employed an 80-min gradient (experimental section) allowing separation of components that were not resolved in the conditions for the Chip/TOF MS. Each HPLC fraction was analyzed further to perform the complete structural elucidation.

Figure 2 is the EIC for FS-LNH isomers found in several HPLC fractions (Figure 2a–g). For reference, Figure 1b is duplicated in the first panel of Figure 2. The figure illustrates the

general approach for elucidating the glycome as well as the efficacy of the methods for separation and structural elucidation. Figures 2a–g show each component as separated by standard HPLC with the HPLC fractions examined by Chip/TOF MS. The inset structures were determined by one of the two methods. (1) For compounds where standards were available retention times and tandem MS were compared with the standards. (2) For the remainder, which was the vast majority, structures were determined by a combination of tandem MS and targeted exoglycosidase digestion. From the group in Figure 2a–g, two compounds were determined by standards obtained commercially, FS-LNH (Figure 2d) and FS-LNnH I (Figure 2f). Among all sialylated OS, 12 standards were identified in this manner. Two new structures were obtained in this group, 4121a (Figure 2a) and 4121b (Figure 2b). The nomenclature is based on the number of hexose (Hex), Fuc, GlcNAc, and NeuAc, respectively. Three structures were elucidated and found to correspond to published structures (Figure 2c, 2e, and 2g) with the names previously assigned.

With PGC as stationary phase, the chip based nano-LC column (43 mm) is generally sufficient to separate isomers using the 45 min gradient. However, under the chosen conditions some isomers such as 4121b and FS-LNH III have similar retention times with 23.9 and 24.0 min, respectively. In this situation, the off-line HPLC column (100 mm) with an 80-min gradient allowed separation of the isomers into different fractions. The isomers in the fractions were injected into Chip/QTOF, which showed two distinct structures based on tandem MS.

Tandem MS Analysis of Sialylated OS

Figure 3a and 3b are MS/MS spectra of a commercial standard FS-LNH. The singly-charged ion m/z 1512.6 yields the tandem MS spectrum in Figure 3a, The doubly-charged ion m/z 756.8 yields the spectrum in Figure 3b. As seen clearly, the doubly-charged species generally provides more structurally informative fragment ions. The following discussions of all the FS-LNH isomers will therefore focus on the MS/MS of the doubly-charged ions. Fragmentation for this ion starts from both non-reducing termini when the HMO has two antennae at the lactose core. In Figure 3b, m/z 756.8 (+2) loses a Fuc to generate m/z 683.8 (+2) and a galactose to generate m/z 602.7 (+2). The subsequent loss of GlcNAc generates m/z 1001.4. This product ion further loses the lactose core to generate m/z 657.2. An alternative fragmentation pathway starts with the loss of NeuAc to generate m/z 1221.5, which is weakly abundant. The further loss of a lactosamine unit [Gal+GlcNAc] from m/z 1221.5 generates m/z 856.3. The following loss of the lactose core generates m/z 512.2. Figure 3c is the tandem spectrum of FS-LNH in HPLC fraction 36 from the milk sample. The FS-LNH from two different sources, with different amounts, yielded nearly identical spectra. Figure 3b and 3c show that even though the total ion intensities (or concentrations) for the two samples are different, the overall features of the tandem MS are nearly identical. In general, when the same collision energy is applied, the resulting tandem MS spectra are highly reproducible.

Structure Elucidation

Elucidation of individual structures begins with the tandem MS. Figure 4 shows the MS/MS spectra for three of FS-LNH isomers, a new glycan 4121a, and two structures that were elucidated and found to correspond to previously published ones, FS-LNH I and FS-LNH II. In Figure 4a, the precursor ion of 4121a m/z 756.8 (+2) loses lactose to yield m/z 1168.4. The fragment ion m/z 1168.4 readily loses a Fuc to generate m/z 1022.4. In Figure 4b and c, the precursor ions of the two other isomers did not yield the analogous fragment ions. Based on this information, it is believed that the new compound 4121a has a linear core structure while the other two both have branched cores, which cannot lose lactose from the quasimolecular ion. In contrast, both structures FS-LNH I and FS-LNH II loses Fuc and a

Gal to generate m/z 602.7 (+2) (weakly abundant in Figure 4c) from the precursor ion, consistent with the presence of Lewis a and \times epitopes at one terminus of each compound. The loss of these residues further confirms the position of NeuAc as being on the other terminus (Figure 4b and c). The same fragment ion is not observed in Figure 4a since 4121a has a linear core and NeuAc at the non-reducing end must fragment before Gal. The differences between FS-LNH I and FS-LNH II are readily determined by several other diagnostic peaks. The fragment peak m/z 495.2 is only found in FS-LNH I, and in none of the other isomers, because sialylation is directly on the GlcNAc (Figure 4b). The Y type ion m/z 1059.4 in FS-LNH II is generated by losing NeuAc (m/z 1221.5) and then Gal. The corresponding B ion m/z 454.2 also indicates the differences in connectivity of NeuAc in both FS-LNH II and FS-LNH I (Figure 4c).

Two isomers with similar retention times, the new OS 4121b and FS-LNH III are readily distinguished based on their tandem MS (Figure 5). The linear compound 4121b yields the fragment ion m/z 1168.4 (and m/z 584.7 (+2)) due to the loss of the lactose. The subsequent loss of a Fuc produces m/z 1022.4 (and m/z 511.7 (+2)) (Figure 5a). An alternative pathway further yields the intense peak m/z 665.7 (+2) due to the loss of the reducing end glucose (Glc) from the quasimolecular ion – also indicating that the Fuc is not on the reducing end. The lack of the diagnostic ion m/z 495.2 (NeuAc-GlcNAc), as shown with FS-LNH I, is indicative that the NeuAc is attached to Gal.

The fragmentation behavior of FS-LNH III also follows several pathways due to its branched core structure (Figure 5b). One of the fragmentation pathways begins with the loss of NeuAc to generate m/z 1221.5. The subsequent loss of a lactosamine unit yielded m/z 856.3. The fragment ion m/z 856.3 further loses lactose to produce m/z 512.2. An alternate pathway starting with the loss of a Fuc yielded m/z 683.7 (+2), followed by a Gal loss to form the product ion m/z 602.7 (+2). The subsequent fragmentation generates m/z 1001.4 by losing a GalNAc and lactose loss to yield m/z 657.2. The complementary information from these two fragmentation pathways also confirm that NeuAc and Fuc are on different branches. However, the generation of m/z 675.8 (+2) and m/z 1147.4 is not consistent with the structure. These ions are the results of the rearrangement of the Fuc within the protonated species.⁵⁸ The exact linkages between the monosaccharides were confirmed with exoglycosidase digestion.

Linkage Elucidation with Exoglycosidase Digestion

The detailed procedure for performing the exoglycosidase digestions is described in previous publications.^{55–56} The conditions in this study for the specific enzyme have been modified and summarized in Supplementary table 2. For convenience the reaction was monitored by MALDI MS. In so doing, the full structure is elucidated by combining MS, tandem MS and the exoglycosidase digestion.

Compounds where no standard is available, the vast majority of the structures, need to be fully elucidated even if the structures have been previously published. The digestion of FS-LNH III (in HPLC fraction 35) is described to provide a more complicated example than 4121b, as the linkages need to be confirmed for both antennae. The results of the digestion for fraction 35 are summarized in Figure 6. Figure 6a is the MALDI MS of HPLC fraction 35 in the positive ion mode before enzyme digestion. As can be seen, the spectrum of FS-LNH III yielded the quasimolecular ion m/z 1556.5 $[M+2Na-H]^+$ and a fragment ion, m/z 1243.4 from the loss of NeuAc. The incubation with $\alpha(2-3)$ -neuraminidase for 1h showed that the presence of $\alpha 2-6$ linkage of NeuAc in this isomer because m/z 1556.5 was not digested (Figure 6b). Figure 6c is the result from the reaction with a non-specific sialidase. After cleaving off the NeuAc from the Gal, a second digestion step with $\beta(1-4)$ -galactosidase generated a new peak, m/z 1081.4, that confirmed the $\beta 1-4$ linkage of Gal

bound to GlcNAc (Figure 6e). The result from this step also indicated that Fuc is present on the other branch. The digestion from the other branch started with $\alpha(1-3,4)$ -fucosidase that generated a new $[M+2Na-H]^+$ ion with m/z 1410.5 (Figure 6d). The result from this step showed that Fuc has $\alpha 1-3,4$ linkage attached to the GlcNAc and not the Gal. In addition, the disappearance of m/z 1243.4 in Figure 6d confirmed that it was a fragment peak from m/z 1556.5 in Figure 6a. The further digestion of m/z 1410.5 by $\beta(1-3)$ -galactosidase generated a new peak m/z 1248.4, which is still a sialylated species (Figure 6f). The result proved a *Lewis a* epitope on the fucosylated antenna. This method was applied to all the other structures.

Negative Mode MS/MS Analysis

In some occasions, it had been necessary to supplement the positive ion MS/MS with negative ion analysis. In the positive ion mode, the fragmentation of the collision activated ions generated primarily *B*, *Y* type ions.⁵⁷ In certain cases, such as FS-LNH and FS-LNnH I, MS/MS yielded the same fragments albeit with great variation in intensities. In this way, tandem MS in the positive mode can be used to identify specific oligosaccharides but not elucidating similar structures (Supplementary Figure 2). However, the fragmentation in the negative ion mode using the Chip/QTOF MS was useful for producing different pathways. In the negative ion mode, our solvent system generated primarily deprotonated ions and formylated ions.⁵⁹ For all FS-LNH isomers, m/z 754.8(-2) $[M-2H]^{2-}$ and m/z 777.8(-2) $[M-H+HCOO]^{2-}$ were both seen in the negative ion mode. The precursor ion m/z 777.8(-2) readily loses formic acid (HCOOH) to generate m/z 754.8(-2) and subsequent fragment ions (Figure 7). In Figure 7a, m/z 754.8(-2) first loses a Fuc to generate a $Z_{4\alpha}$ ion with m/z 1346.5. The subsequent loss of Gal yields $Z_{3\alpha}$ with m/z 1184.4. While in Figure 7b, m/z 754.8(-2) loses a Fuc to produce $Z_{3\beta}$, then a following Gal loss yielded $Z_{3\beta/13\beta}$. Since Fuc and Gal both link to GalNAc, the Gal loss may occur before Fuc loss to generate the $Z_{3\beta}$, which is not found in Figure 7a since Fuc links to Gal at the reducing end in FS-LNH. In this case, the fragmentation in the negative ion mode provides a better way to resolve the connectivity between the two isomers. The structure information from the negative mode MS/MS was therefore, at times, a necessary complement to the positive ion mode.

Discussion

30 SHMO structures with retention time and mass are listed in Table 2. This table along with the tandem MS is valuable for rapidly identifying known structures. Comparison of the retention time and the tandem MS provides a highly specific method for identifying oligosaccharides. When combined with previously determined neutral HMOs,³⁶ a library with over 70 structures is constructed which incorporates nano-LC retention time, accurate mass, and MS/MS spectra.

Based on the structures, we find a few general observations regarding sialylation in HMOs. Note that these observations are based on a pool of samples from five mothers.

1. The majority of the SHMOs are mono-sialylated (90.9 %) with the smaller fraction being di-sialylated (9.1 %). (Supplementary Figure 3)
2. The more abundant linkage corresponds to $\alpha 2-6$ (56.9%), while only 4.8% SHMOs were found with $\alpha 2-3$ NeuAc by far. (Supplementary Figure 3)
3. The $\alpha 2-3$ NeuAc is usually bound to a $\beta 1-3$ galactose, except for sialyl lactose.
4. The $\alpha 2-6$ NeuAc is usually bound to $\beta 1-4$ galactose.

5. Sialylation on the GlcNAc is only found as α 2-6 linkage as previously reported.^{2,35} However, this arrangement is even more specifically found only on the β 1-3 branch from the core lactose.

The method for elucidating structure employing tandem MS and exoglycosidase is generally successful with a caveat. Examination of the different fragmentation pathways from various protonated isomers showed rearrangements that can affect the interpretation. For example, the compound FS-LNH generates fragment ion m/z 675.8(+2) by losing a Gal, which is not consistent with the structure (Figure 3b and 3c). This rearrangement is caused by the long-range migration of the Fuc, most likely to a hydroxyl group of the reducing end residue.^{58,70–71} Similar rearrangements are not observed for sodiated ions in MALDI FTICR when performing CID or IRMPD experiments as noted previously.^{36,58} In order to confirm the connectivity and linkages of monosaccharides, exoglycosidase digestion was necessary to validate the structural information obtained from tandem MS.

The future work will be imputing all the retention times and MS/MS spectra with all the elucidated structures into Agilent Masshunter software. Auto MS/MS search will be performed by the software for the unknown HMO samples and compared with the spectra in the database. An output of the compound list will include all the identified structures with the matching scores. This library will eventually provide a high-throughput method for oligosaccharide analysis.

Supplementary Material

Refer to Web version on PubMed Central for supplementary material.

Acknowledgments

Funding provided by the National Institutes of Health (HD059127 and HD061923), UC Discovery, and the California Dairy Research Fund are gratefully acknowledged.

References

1. Kunz C, Rudloff S, Baier W, Klein N, Strobel S. Oligosaccharides in human milk: Structural, functional, and metabolic aspects. *Annu Rev Nutr.* 2000; 20:699–722. [PubMed: 10940350]
2. Boehm, G.; Stahl, B. *Functional Dairy Products*. Cambridge, England: CRC Press; 2003. p. 203
3. Dai DW, Nanthkumar NN, Newburg DS, Walker WA. Role of oligosaccharides and glycoconjugates in intestinal host defense. *J Pediatr Gastr Nutr.* 2000; 30:S23–S33.
4. Newburg DS, Ruiz-Palacios GM, Morrow AL. Human milk glycans protect infants against enteric pathogens. *Annu Rev Nutr.* 2005; 25:37–58. [PubMed: 16011458]
5. Boehm G, Stahl B. Oligosaccharides from milk. *J Nutr.* 2007; 137(3):847S–849S. [PubMed: 17311985]
6. Ninonuevo MR, Park Y, Yin HF, Zhang JH, Ward RE, Clowers BH, German JB, Freeman SL, Killeen K, Grimm R, Lebrilla CB. A strategy for annotating the human milk glycome. *J Agr Food Chem.* 2006; 54(20):7471–7480. [PubMed: 17002410]
7. Bode L, Kunz C, Muhly-Reinholz M, Mayer K, Seeger W, Rudolf S. Inhibition of monocyte, lymphocyte, and neutrophil adhesion to endothelial cells by human milk oligosaccharides. *Thromb Haemost.* 2004; 92:1402–1410. [PubMed: 15583750]
8. Varki A. Sialic acids in human health and disease. *Trends Mol Med.* 2008; 14(8):351–360. [PubMed: 18606570]
9. Idota T, Kawakami H, Murakami Y, Sugawara M. Inhibition of Cholera-Toxin by Human-Milk Fractions and Sialyllactose. *Biosci Biotech Bioch.* 1995; 59(3):417–419.

10. Virkola R, Parkkinen J, Hacker J, Korhonen TK. Sialyloligosaccharide Chains of Laminin as an Extracellular-Matrix Target for S Fimbriae of Escherichia-Coli. *Infect Immun*. 1993; 61(10):4480–4484. [PubMed: 8104897]
11. Schnaar RL. Glycolipid-mediated cell-cell recognition in inflammation and nerve regeneration. *Arch Biochem Biophys*. 2004; 426(2):163–172. [PubMed: 15158667]
12. Varki A. Glycan-based interactions involving vertebrate sialic-acid-recognizing proteins. *Nature*. 2007; 446(7139):1023–1029. [PubMed: 17460663]
13. Varki A, Angata T. Siglecs - the major subfamily of I-type lectins. *Glycobiology*. 2006; 16(1):1R–27R. [PubMed: 16118287]
14. Johnson CP, Fujimoto I, Rutishauser U, Leckband DE. Direct evidence that neural cell adhesion molecule (NCAM) polysialylation increases intermembrane repulsion and abrogates adhesion. *J Biol Chem*. 2005; 280(1):137–145. [PubMed: 15504723]
15. El Maarouf A, Petridis AK, Rutishauser U. Use of polysialic acid in repair of the central nervous system. *P Natl Acad Sci USA*. 2006; 103(45):16989–16994.
16. Morrow AL, Ruiz-Palacios GM, Jiang X, Newburg DS. Human-milk glycans that inhibit pathogen binding protect breast-feeding infants against infectious diarrhea. *J Nutr*. 2005; 135(5):1304–1307. [PubMed: 15867329]
17. Wang B, McVeagh P, Petocz P, Brand-Miller J. Brain ganglioside and glycoprotein sialic acid in breastfed compared with formula-fed infants. *Am J Clin Nutr*. 2003; 78(5):1024–1029. [PubMed: 14594791]
18. An HJ, Lebrilla C. Structure Elucidation of Native N- and O-linked Glycans by Tandem Mass Spectrometry. *Mass Spectrom Rev*. 2010 In Press.
19. Toyoda M, Ito H, Matsuno YK, Narimatsu H, Kameyama A. Quantitative derivatization of sialic acids for the detection of sialoglycans by MALDI MS. *Anal Chem*. 2008; 80(13):5211–5218. [PubMed: 18484736]
20. Harvey DJ. Matrix-Assisted Laser Desorption/Ionization Mass Spectrometry of Carbohydrates. *Mass Spectrom Rev*. 1999; 18:349–451. [PubMed: 10639030]
21. Lattova E, Snovida S, Perreault H, Krokhin O. Influence of the labeling group on ionization and fragmentation of carbohydrates in mass spectrometry. *J Am Soc Mass Spectr*. 2005; 16(5):683–696.
22. Delaney J, Vouros P. Liquid chromatography ion trap mass spectrometric analysis of oligosaccharides using permethylated derivatives. *Rapid Commun Mass Sp*. 2001; 15(5):325–334.
23. Morelle W, Slomianny MC, Diemer H, Schaeffer C, van Dorsselaer A, Michalski JC. Fragmentation characteristics of permethylated oligosaccharides using a matrix-assisted laser desorption/ionization two-stage time-of-flight (TOF/TOF) tandem mass spectrometer. *Rapid Commun Mass Sp*. 2004; 18(22):2637–2649.
24. Wheeler SF, Domann P, Harvey DJ. Derivatization of sialic acids for stabilization in matrix-assisted laser desorption/ionization mass spectrometry and concomitant differentiation of alpha(2 - > 3)- and alpha(2 - > 6)-isomers. *Rapid Commun Mass Sp*. 2009; 23(2):303–312.
25. Powell AK, Harvey DJ. Stabilization of sialic acids in N-linked oligosaccharides and gangliosides for analysis by positive ion matrix-assisted laser desorption ionization mass spectrometry. *Rapid Commun Mass Sp*. 1996; 10(9):1027–1032.
26. Mattu TS, Royle L, Langridge J, Wormald MR, Van den Steen PE, Van Damme J, Opendakker G, Harvey DJ, Dwek RA, Rudd PM. O-glycan analysis of natural human neutrophil gelatinase B using a combination of normal phase- HPLC and online tandem mass spectrometry: Implications for the domain organization of the enzyme. *Biochemistry-U.S.* 2000; 39(51):15695–15704.
27. Harvey DJ. Collision-induced fragmentation of negative ions from N-linked glycans derivatized with 2-aminobenzoic acid. *J Mass Spectrom*. 2005; 40(5):642–653. [PubMed: 15751107]
28. Pikulski M, Hargrove A, Shabbir SH, Anslyn EV, Brodbelt JS. Sequencing and characterization of oligosaccharides using infrared multiphoton dissociation and boronic acid derivatization in a quadrupole ion trap. *J Am Soc Mass Spectr*. 2007; 18(12):2094–2106.
29. Amano J, Sugahara D, Osumi K, Tanaka K. Negative-ion MALDI-QIT-TOFMSn for structural determination of fucosylated and sialylated oligosaccharides labeled with a pyrene derivative. *Glycobiology*. 2009; 19(6):592–600. [PubMed: 19240273]

30. Novotny MV, Mechref Y. New hyphenated methodologies in high-sensitivity glycoprotein analysis. *J Sep Sci.* 2005; 28(15):1956–1968. [PubMed: 16276785]
31. Takegawa Y, Deguchi K, Keira T, Ito H, Nakagawa H, Nishimura S. Separation of isomeric 2-aminopyridine derivatized N-glycans and N-glycopeptides of human serum immunoglobulin G by using a zwitterionic type of hydrophilic-interaction chromatography. *J Chromatogr A.* 2006; 1113(1–2):177–181. [PubMed: 16503336]
32. Wuhler M, Koeleman CAM, Deelder AM, Hokke CN. Normal-phase nanoscale liquid chromatography - Mass spectrometry of underivatized oligosaccharides at low-femtomole sensitivity. *Anal Chem.* 2004; 76(3):833–838. [PubMed: 14750882]
33. Thurl S, MullerWerner B, Sawatzki G. Quantification of individual oligosaccharide compounds from human milk using high-pH anion-exchange chromatography. *Anal Biochem.* 1996; 235(2): 202–206. [PubMed: 8833329]
34. Coppa GV, Pierani P, Zampini L, Carloni I, Carlucci A, Gabrielli O. Oligosaccharides in human milk during different phases of lactation. *Acta Paediatr.* 1999; 88:89–94. [PubMed: 10090555]
35. Finke B, Stahl B, Pfenninger A, Karas M, Daniel H, Sawatzki G. Analysis of high-molecular-weight oligosaccharides from human milk by liquid chromatography and MALDI-MS. *Anal Chem.* 1999; 71(17):3755–3762. [PubMed: 10489525]
36. Wu S, Tao N, German B, Grimm R, Lebrilla C. Development of an Annotated Library of Neutral Human Milk Oligosaccharides. *J Proteome Res.* 2010; 9(8):4138–4151. [PubMed: 20578730]
37. Koizumi K. High-performance liquid chromatographic separation of carbohydrates on graphitized carbon columns. *J Chromatogr A.* 1996; 720(1–2):119–126. [PubMed: 8601188]
38. Pabst M, Altmann F. Influence of electrosorption, solvent, temperature, and ion polarity on the performance of LC-ESI-MS using graphitic carbon for acidic oligosaccharides. *Anal Chem.* 2008; 80(19):7534–7542. [PubMed: 18778038]
39. Ruhaak LR, Deelder AM, Wuhler M. Oligosaccharide analysis by graphitized carbon liquid chromatography-mass spectrometry. *Anal Bioanal Chem.* 2009; 394(1):163–174. [PubMed: 19247642]
40. Guile GR, Rudd PM, Wing DR, Prime SB, Dwek RA. A rapid high-resolution high-performance liquid chromatographic method for separating glycan mixtures and analyzing oligosaccharide profiles. *Anal Biochem.* 1996; 240(2):210–226. [PubMed: 8811911]
41. Tao N. Structural determination and daily variations of porcine milk oligosaccharides. *J Agr Food Chem.* 2010; 58:4653–4659. [PubMed: 20369835]
42. Karlsson NG, Wilson NL, Wirth HJ, Dawes P, Joshi H, Packer NH. Negative ion graphitised carbon nano-liquid chromatography/mass spectrometry increases sensitivity for glycoprotein oligosaccharide analysis. *Rapid Commun Mass Sp.* 2004; 18(19):2282–2292.
43. Zhao J, Qiu WL, Simeone DM, Lubman DM. N-linked glycosylation profiling of pancreatic cancer serum using capillary liquid phase separation coupled with mass spectrometric analysis. *J Proteome Res.* 2007; 6(3):1126–1138. [PubMed: 17249709]
44. Harvey DJ. Collision-induced fragmentation of underivatized N-linked carbohydrates ionized by electrospray. *J Mass Spectrom.* 2000; 35(10):1178–1190. [PubMed: 11110090]
45. Harvey DJ. Fragmentation of negative ions from carbohydrates: Part 1. Use of nitrate and other anionic adducts for the production of negative ion electrospray spectra from N-linked carbohydrates. *J Am Soc Mass Spectr.* 2005; 16(5):622–630.
46. Harvey DJ. Fragmentation of negative ions from carbohydrates: Part 2. Fragmentation of high-mannose N-linked glycans. *J Am Soc Mass Spectr.* 2005; 16(5):631–646.
47. Harvey DJ. Fragmentation of negative ions from carbohydrates: Part 3. Fragmentation of hybrid and complex N-linked glycans. *J Am Soc Mass Spectr.* 2005; 16(5):647–659.
48. Zhang JH, Schubothe K, Li BS, Russell S, Lebrilla CB. Infrared multiphoton dissociation of O-linked mucin-type oligosaccharides. *Anal Chem.* 2005; 77(1):208–214. [PubMed: 15623298]
49. Lancaster KS, An HJ, Li BS, Lebrilla CB. Interrogation of N-linked oligosaccharides using infrared multiphoton dissociation in FT-ICR mass spectrometry. *Anal Chem.* 2006; 78(14):4990–4997. [PubMed: 16841922]

50. Devakumar A, Mechref Y, Kang P, Novotny MV, Reilly JP. Laser-induced photofragmentation of neutral and acidic glycans inside an ion-trap mass spectrometer. *Rapid Commun Mass Sp.* 2007; 21(8):1452–1460.
51. Adamson JT, Hakansson K. Electron capture dissociation of oligosaccharides ionized with alkali, alkaline earth, and transition metals. *Anal Chem.* 2007; 79(7):2901–2910. [PubMed: 17328529]
52. Adamson JT, Hakansson K. Electron detachment dissociation of neutral and sialylated oligosaccharides. *J Am Soc Mass Spectr.* 2007; 18(12):2162–2172.
53. Mechref Y, Novotny MV, Krishnan C. Structural characterization of oligosaccharides using MALDI-TOF/TOF tandem mass spectrometry. *Anal Chem.* 2003; 75(18):4895–4903. [PubMed: 14674469]
54. Lewandrowski U, Resemann A, Sickmann A. Laser-induced dissociation/high-energy collision-induced dissociation fragmentation using MALDI-TOF/TOF-MS instrumentation for the analysis of neutral and acidic oligosaccharides. *Anal Chem.* 2005; 77(10):3274–3283. [PubMed: 15889919]
55. Xie YM, Tseng K, Lebrilla CB, Hedrick JL. Targeted use of exoglycosidase digestion for the structural elucidation of neutral O-linked oligosaccharides. *J Am Soc Mass Spectr.* 2001; 12(8): 877–884.
56. Zhang JH, Lindsay LL, Hedrick JL, Lebrilla CB. Strategy for profiling and structure elucidation of mucin-type oligosaccharides by mass spectrometry. *Anal Chem.* 2004; 76(20):5990–6001. [PubMed: 15481946]
57. Domon B, Costello CE. A Systematic Nomenclature for Carbohydrate Fragmentations in Fab-Ms Ms Spectra of Glycoconjugates. *Glycoconjugate J.* 1988; 5(4):397–409.
58. Franz AH, Lebrilla CB. Evidence for long-range glycosyl transfer reactions in the gas phase. *J Am Soc Mass Spectr.* 2002; 13(4):325–337.
59. Antonio C, Pinheiro C, Chaves MM, Ricardo CP, Ortuno MF, Thomas-Oates J. Analysis of carbohydrates in *Lupinus albus* stems on imposition of water deficit, using porous graphitic carbon liquid chromatography-electrospray ionization mass spectrometry (vol 1187, pg 111, 2008). *J Chromatogr A.* 2008; 1201(1):132–132.
60. Kuhn R, Brossmer R. Über Das Durch Viren Der Influenza-Gruppe Spaltbare Trisaccharid Der Milch. *Chem Ber-Recl.* 1959; 92(7):1667–1671.
61. Kuhn R, Gauhe A. Bestimmung Der Bindungsstelle Von Sialinsaureresten in Oligosacchariden Mit Hilfe Von Perjodat. *Chem Ber-Recl.* 1965; 98(2):395–413.
62. Kuhn R, Gauhe A. Die Konstitution Der Lacto-N-Neotetraose. *Chem Ber-Recl.* 1962; 95(2):518–522.
63. Smith DF, Prieto PA, McCrumb DK, Wang WC. A Novel Sialylfucopentaose in Human-Milk - Presence of This Oligosaccharide Is Not Dependent on Expression of the Secretor or Lewis Fucosyltransferases. *J Biol Chem.* 1987; 262(25):12040–12047. [PubMed: 3624247]
64. Grimmonp L, Montreui J. Physical Chemistry of Six New Oligosides Isolated from Human Milk. *B Soc Chim Biol.* 1968; 50(4):843–855.
65. Kobata A, Ginsburg V. Oligosaccharides of Human Milk .3. Isolation and Characterization of a New Hexasaccharide, Lacto-N-Hexaose. *J Biol Chem.* 1972; 247(5):1525–&. [PubMed: 5012321]
66. Gronberg G, Lipniunas P, Lundgren T, Erlansson K, Lindh F, Nilsson B. Human-Milk Oligosaccharides .1. Isolation of Monosialylated Oligosaccharides from Human-Milk and Structural-Analysis of 3 New Compounds. *Carbohydr Res.* 1989; 191(2):261–278.
67. Gronberg G, Lipniunas P, Lundgren T, Lindh F, Nilsson B. Structural-Analysis of 5 New Monosialylated Oligosaccharides from Human-Milk. *Arch Biochem Biophys.* 1992; 296(2):597–610. [PubMed: 1632647]
68. Yamashita K, Tachibana Y, Kobata A. Oligosaccharides of Human Milk .10. Structural Studies of 2 New Octasaccharides, Difucosyl Derivatives of Para-Lacto-N-Hexaose and Para-Lacto-N-Neohexaose. *J Biol Chem.* 1977; 252(15):5408–5411. [PubMed: 885859]
69. Kitagawa H, Nakada H, Fukui S, Funakoshi I, Kawasaki T, Yamashina I, Tate S, Inagaki F. Novel Oligosaccharides with the Sialyl-Le(a) Structure in Human-Milk. *J Biochem-Tokyo.* 1993; 114(4): 504–508. [PubMed: 8276760]

70. Ernst B, Muller DR, Richter WJ. False sugar sequence ions in electrospray tandem mass spectrometry of underivatized sialyl-Lewis-type oligosaccharides. *International Journal of Mass Spectrometry and Ion Processes*. 1997; 160(1–3):283–290.
71. Olsthoorn MMA, Lopez-Lara IM, Petersen BO, Bock K, Haverkamp J, Spaink HP, Thomas-Oates JE. Novel branched nod factor structure results from alpha-(1 -> 3) fucosyl transferase activity: The major lipo-chitin oligosaccharides from *Mesorhizobium loti* strain NZP2213 bear an alpha-(1 -> 3) fucosyl substituent on a nonterminal backbone residue. *Biochemistry-U.S.* 1998; 37(25): 9024–9032.

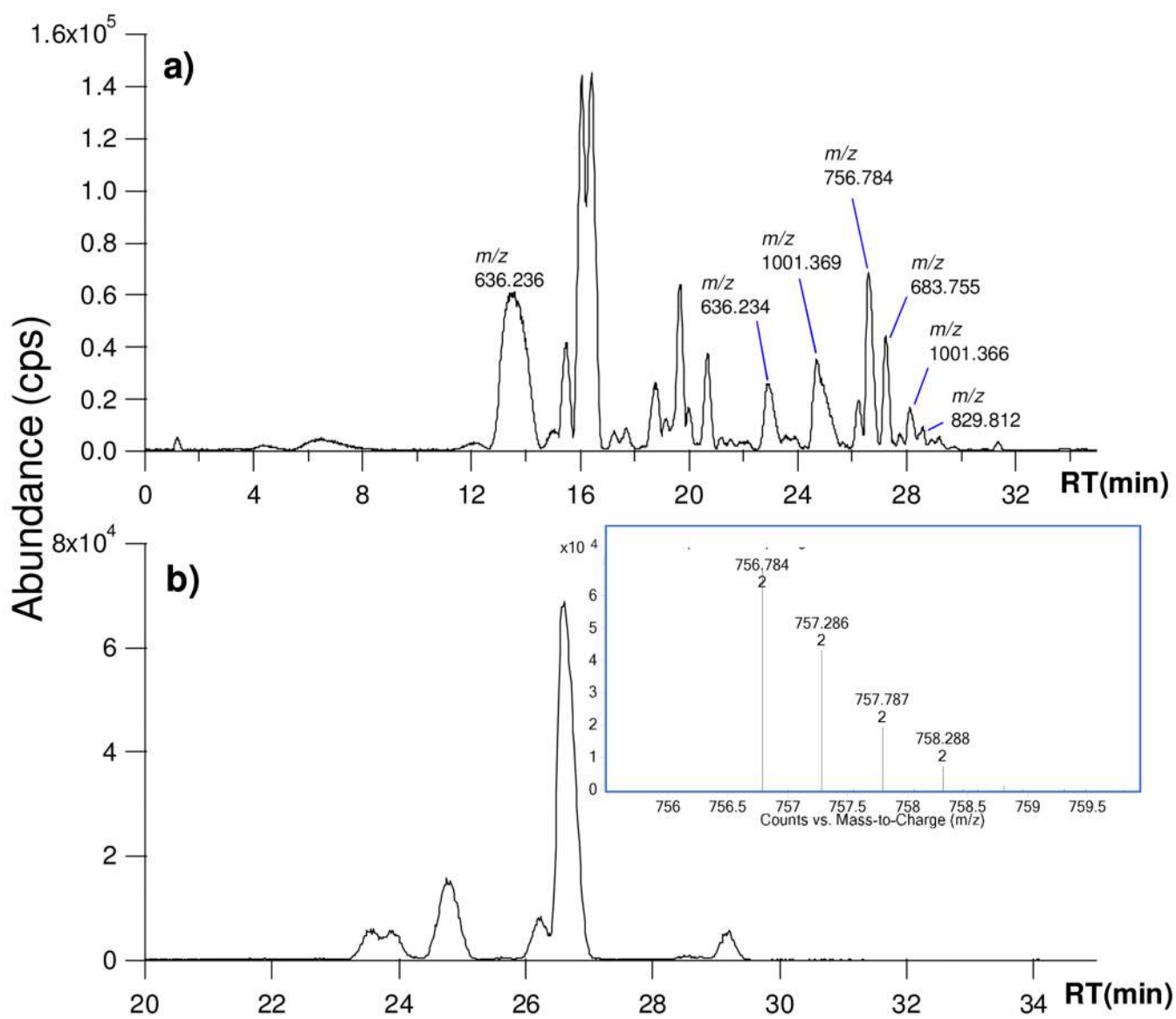


Figure 1.
(a) Base peak chromatogram (BPC) of enriched sialylated human milk oligosaccharides (SHMOs). (b) Extracted ion chromatogram (EIC) of isomers with neutral mass 1511.6 (with MS inset).

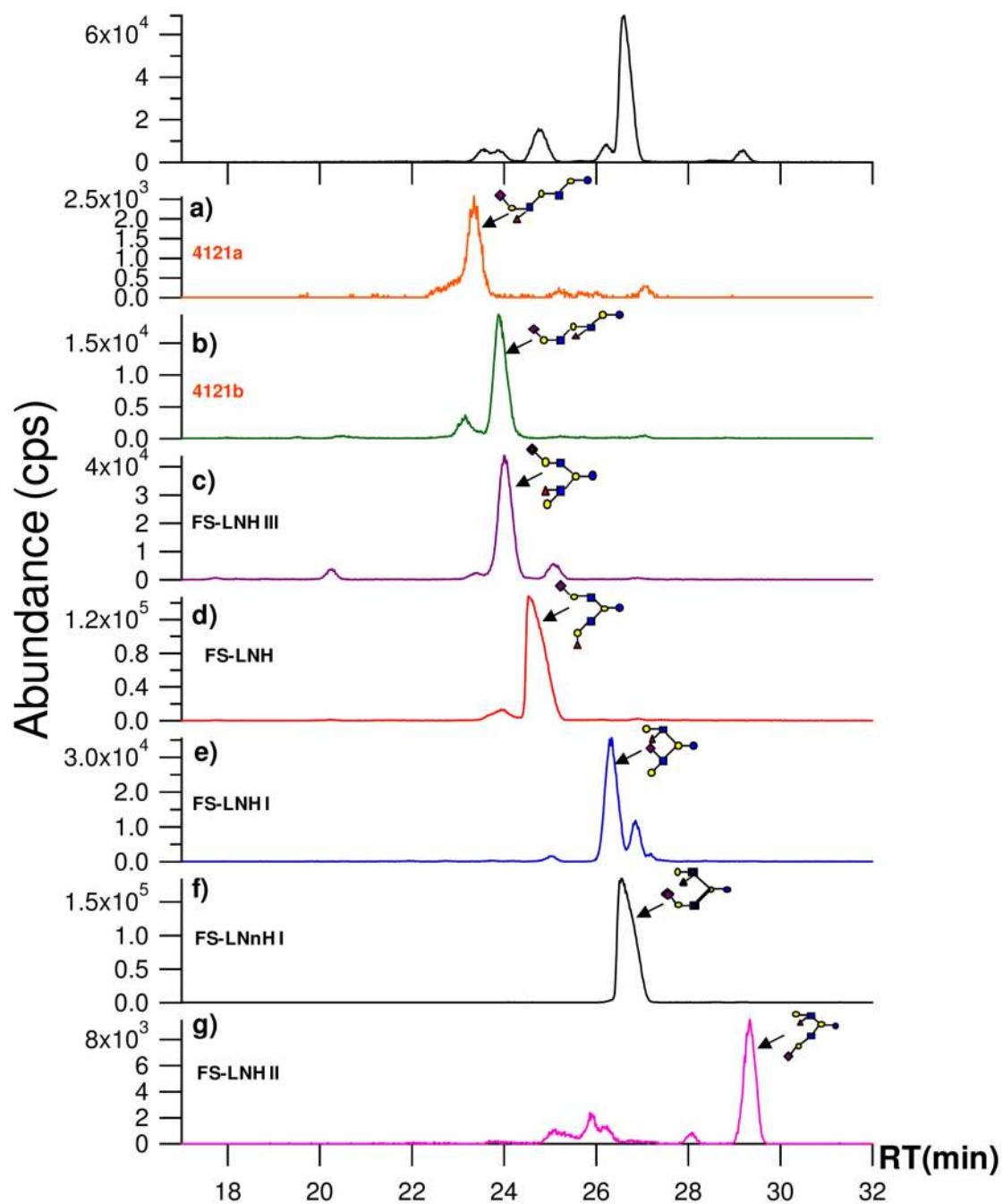
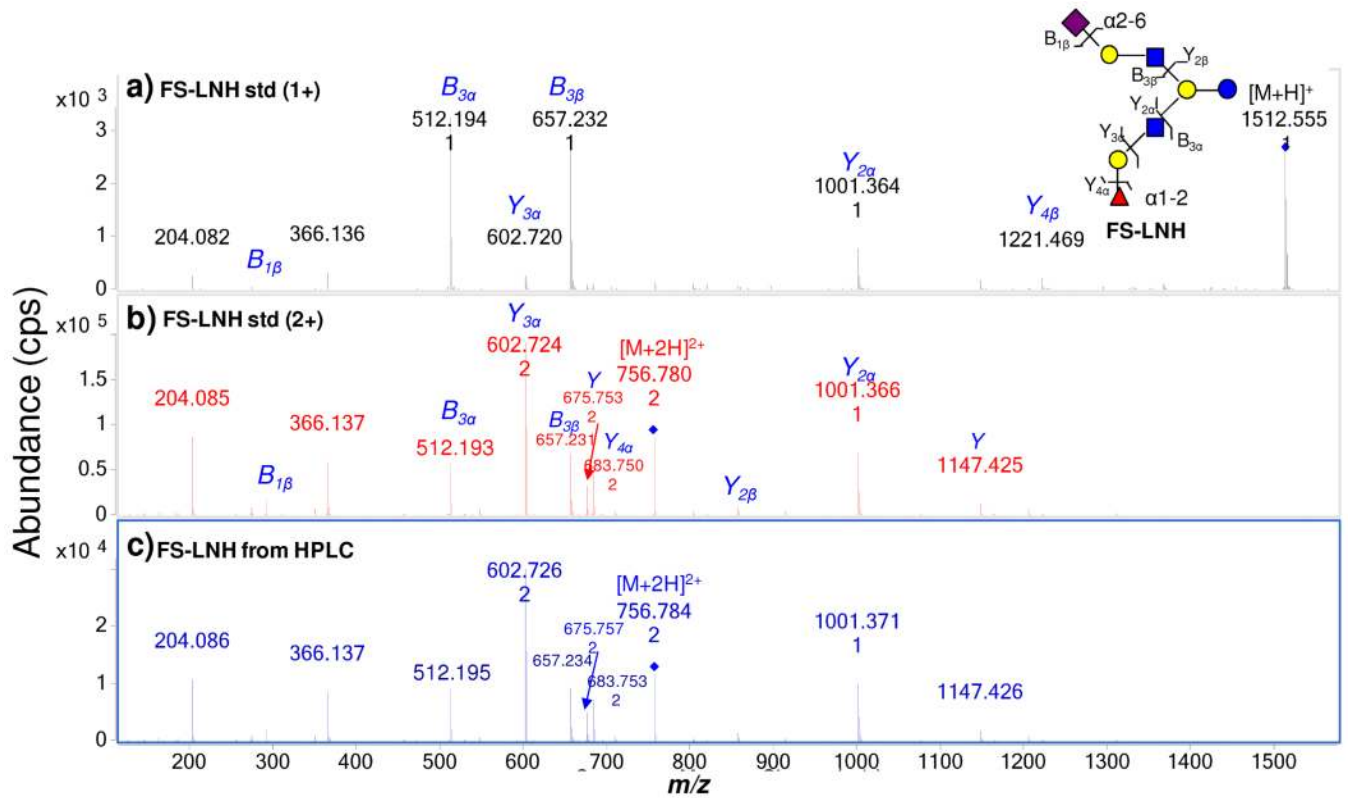


Figure 2. FS-LNH isomers in human milk. The isomers were separated into different fractions using standard HPLC. The selected fractions were then analyzed by Chip/TOF MS (a–g). The structures (inset) were determined as described in the text.

**Figure 3.**

(a) MS/MS of a commercial standard FS-LNH from singly-charged precursor ion (m/z 1512.6). (b) MS/MS of doubly-charged precursor ion (m/z 756.8). (c) MS/MS of FS-LNH obtained from human milk by HPLC fractionation.

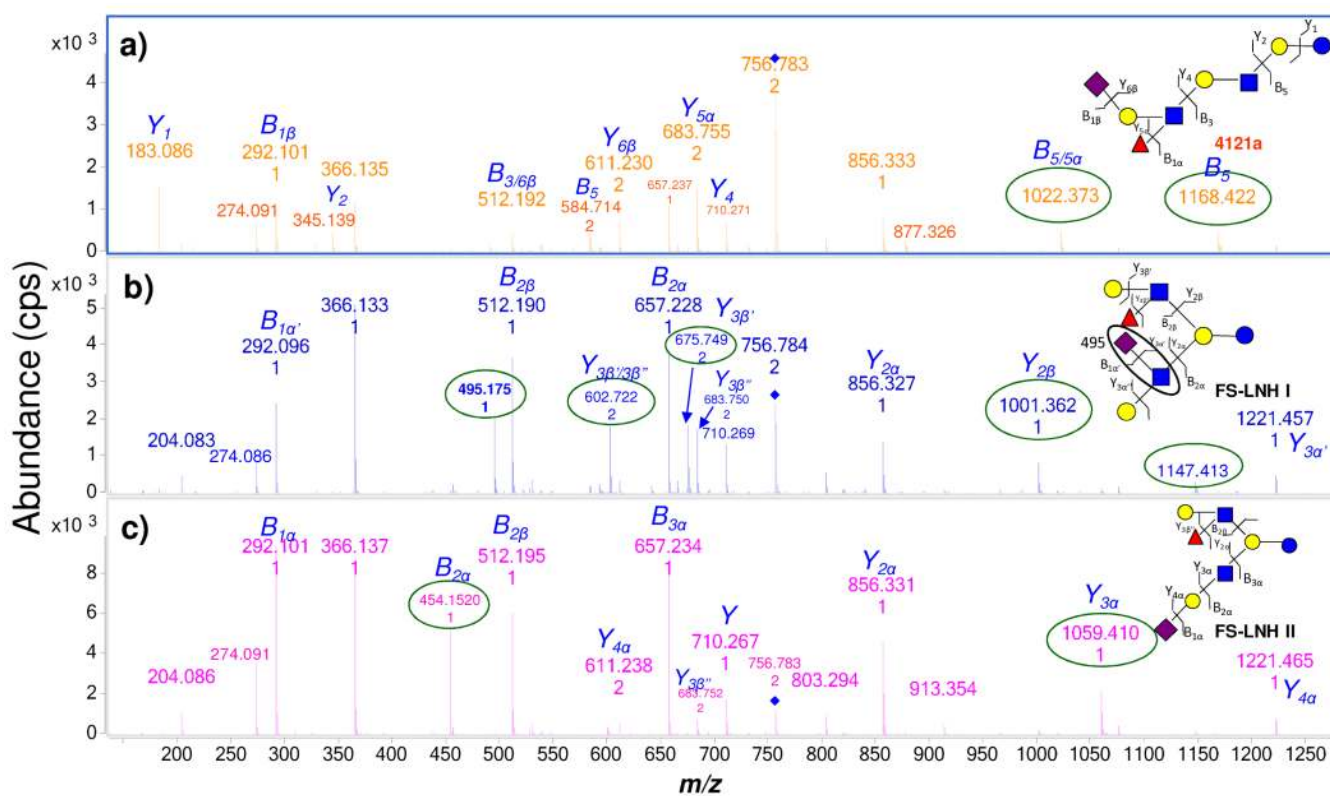


Figure 4. Three isomers - 4121a, FS-LNH I, and FS-LNH II, were differentiated by MS/MS under the identical collision energy. Diagnostic peaks (circled) belong only to the specific isomer.

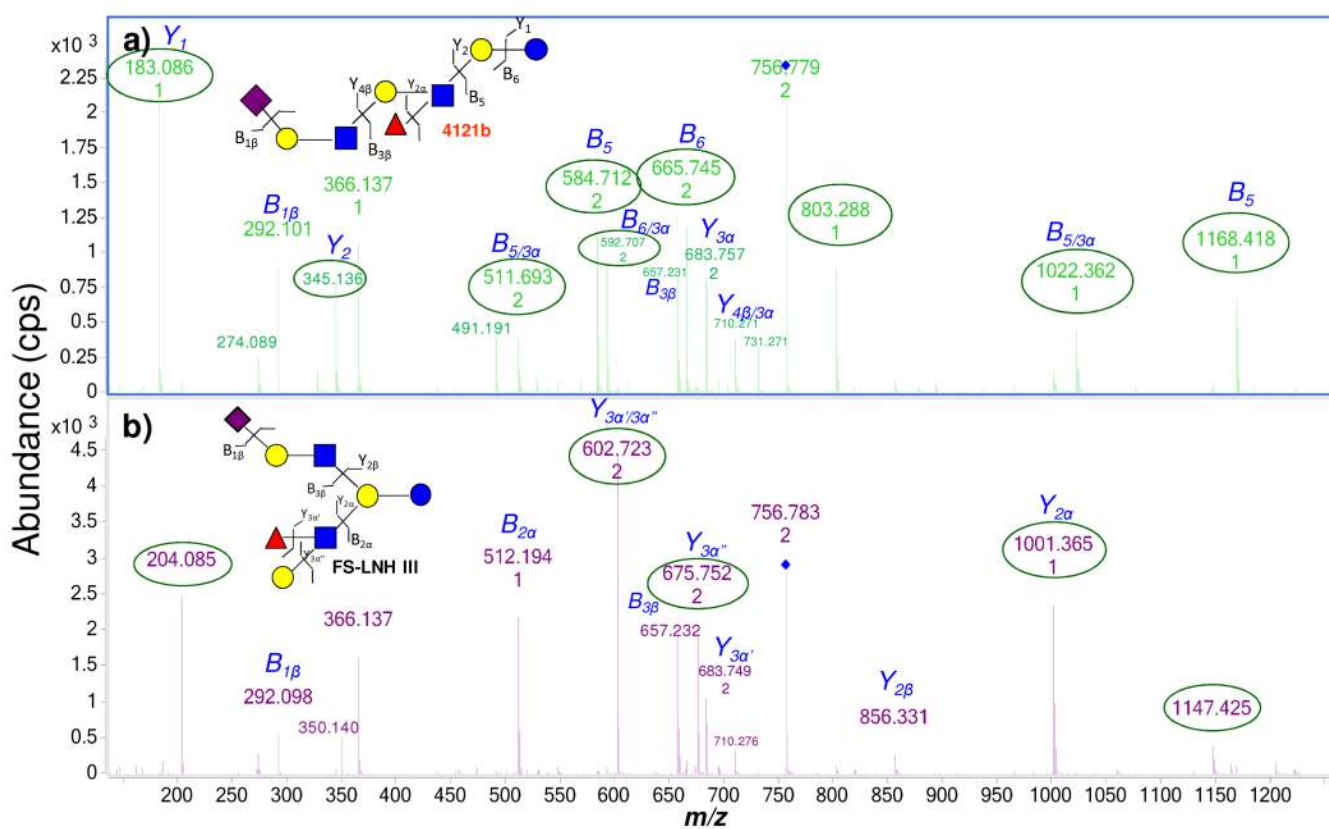


Figure 5. MS/MS spectra serve to distinguish the two isomers – 4121b and FS-LNH III, with nearly identical retention time. Different fragmentation pathways elucidate linear from branched core structures.

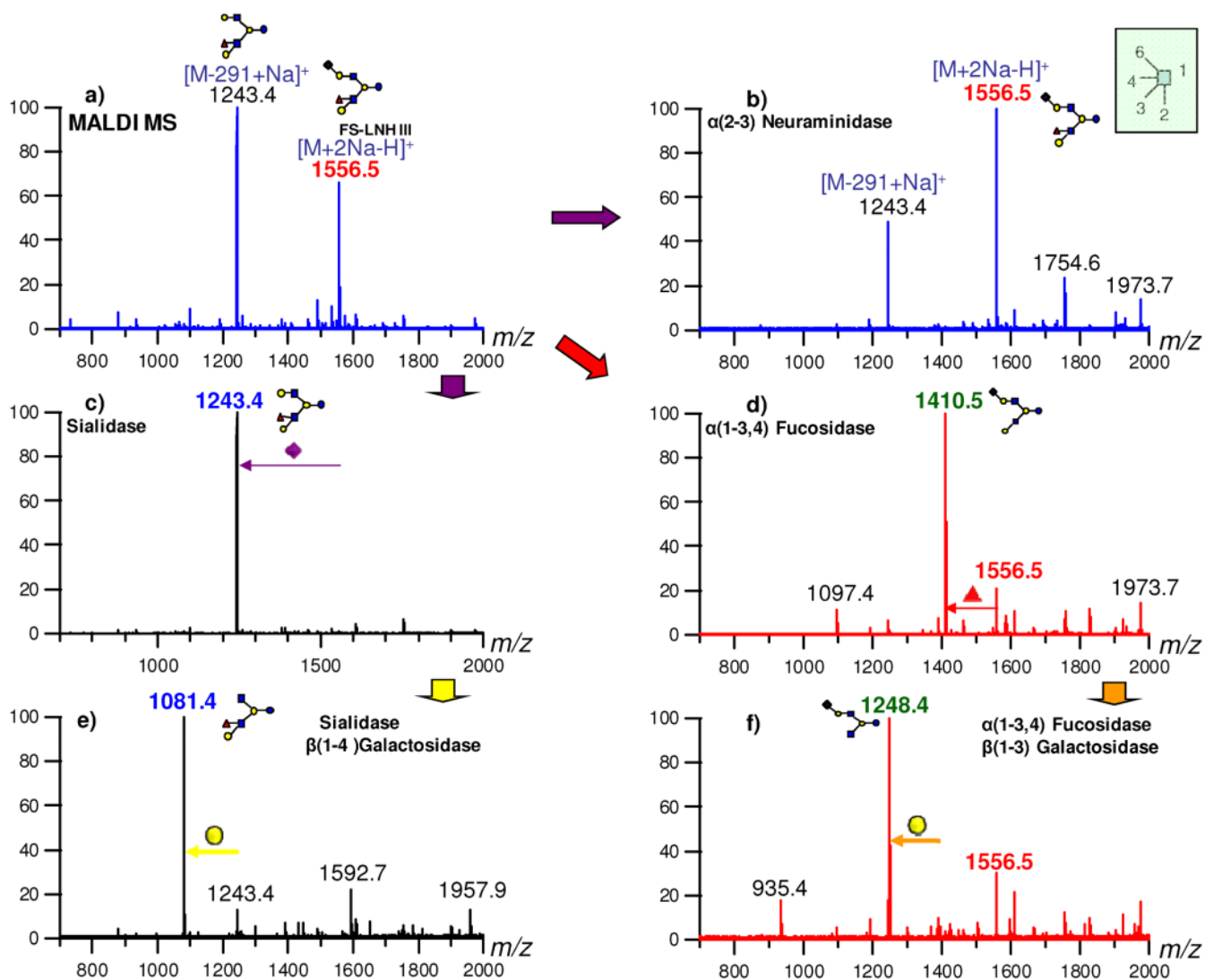


Figure 6.
Exoglycosidase digestion to determine the structure of FS-LNH III found in HPLC fraction 35.

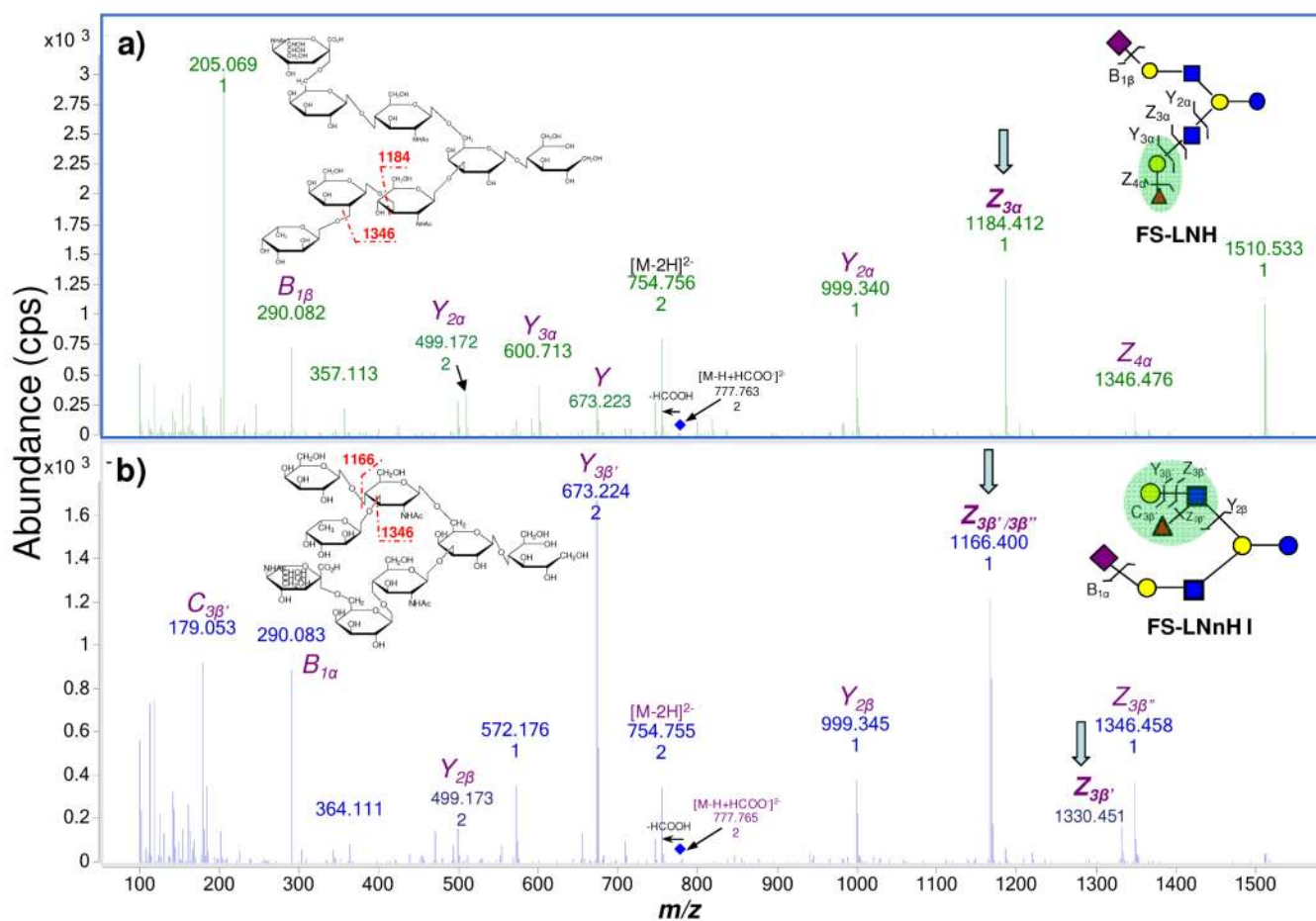


Figure 7. MS/MS spectra of FS-LNH and FS-LNnH I in the negative ion mode. Z type ions can be used to elucidate the different connectivity within the two isomers.

Table 1



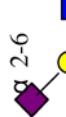

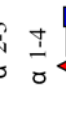

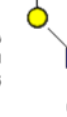
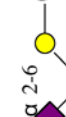

FS-LNH isomers detected by Chip/TOF from enriched SHMOs.


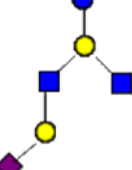

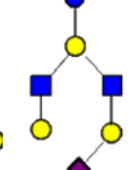
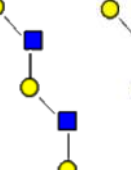
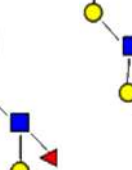
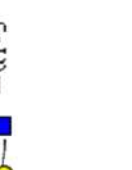
SHMOs	Mass (exptl)	Mass (calcd)	Error (Da)	Hex	Fuc	GlcNAc	NeuAc	RT (min)	Abundance
4121a	1511.547	1511.550	-0.003	4	1	2	1	23.6	255 511
4121b								23.9	
FS-LNH III	1511.553	1511.550	0.003	4	1	2	1	24.0	226 932
FS-LNH	1511.554	1511.550	0.004	4	1	2	1	24.8	771 332
FS-LNH I	1511.552	1511.550	0.002	4	1	2	1	26.2	286 110
FS-LNnH I	1511.554	1511.550	0.004	4	1	2	1	26.6	2 883 226
FS-LNH II	1511.550	1511.550	0.000	4	1	2	1	29.2	206 722

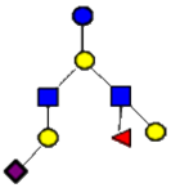
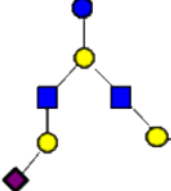
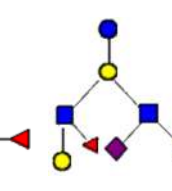
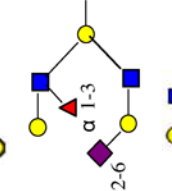
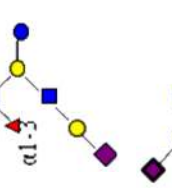
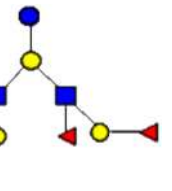
* the abundance is from HPLC-Chip/TOF counts per second (cps)

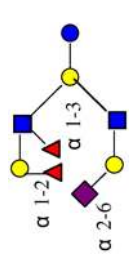
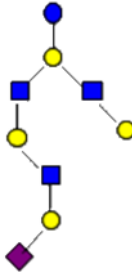
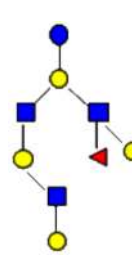
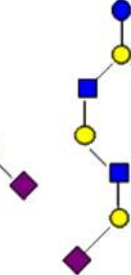
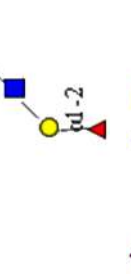
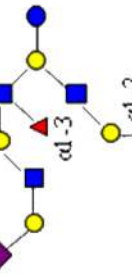
Table 2

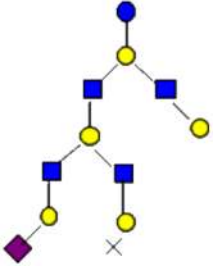
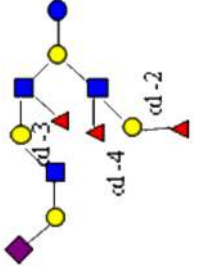
30 SHMO structures determined by Chip/QTOF MS with 10 new OS.

#	Name	Mass (exptl)	Composition	TOF RT (min)	QTOF RT (min)	Structure	Ref
1	6'SL	635.229	2001	13.6	14.6		60
2	3'SL	635.227	2001	22.9	22.6		60
3	6'SLN	676.254	1011	13.1	14.5		61
4	3'SLN	676.252	1011	23.1	23.7		
5	3'Sle ^a	822.314	1111	14.6	12.9		
6	LST ^c	1000.365	3011	24.5	23.8		62
7	LST ^b	1000.365	3011	25.5	24.7		62
8	LST ^a	1000.362	3011	28.1	26.8		62
9	F-LST ^c	1146.419	3111	24.3	23.5		63

#	Name	Mass (exptl)	Composition	TOF RT (min)	QTOF RT (min)	Structure	Ref
10	DSLNT	1291.446	3012	31.2	33.7		64
11	S-LNH	1365.495	4021	26.2	25.3		65
12	4021a	1365.494	4021	27.1	26.1		66
13	S-LNnH II	1365.494	4021	27.3	26.3		
14	4021b	1365.491	4021	29.0	27.9		
15	4121a	1511.547	4121	23.6	22.8		
16	4121b	1511.553	4121	23.9	23.1		

#	Name	Mass (exptl)	Composition	TOF RT (min)	QTOF RT (min)	Structure	Ref
17	FS-LNH III	1511.553	4121	24.0	23.2		67
18	FS-LNH	1511.554	4121	24.8	24.3		68
19	FS-LNH I	1511.552	4121	26.2	25.2		67
20	FS-LNnH I	1511.554	4121	26.6	25.5		66
21	FS-LNH II	1511.550	4121	29.2	27.2		67
22	DFS-LNH	1657.612	4221	24.6	23.7		67

#	Name	Mass (exptl)	Composition	TOF RT (min)	QTOF RT (min)	Structure	Ref
23	DFS-LNnH	1657.608	4221	28.6	27.2		67
24	5031a	1730.622	5031	29.1	27.8		
25	FS-LNO	1876.682	5131	27.2	26.0		69
26	5131a	1876.682	5131	27.9	26.7		
27	5231a	2022.741	5231	26.5	25.4		
28	5231b	2022.739	5231	27.3	26.0		

#	Name	Mass (expt)	Composition	TOF RT (min)	QTOF RT (min)	Structure	Ref
29	6041a	2095.757	6041	29.3	27.8		
30	5331a	2168.803	5331	26.1	25.1		

New structures are indicated in red, for example 4021a. Monosaccharide composition 4Hex:0Fuc:2HexNAc:1NeuAc represented as 4021 with a, b, c, ... as the order of OS from LC.

